IOP Conf. Series: Journal of Physics: Conf. Series **864** (2017) 012028 doi:10.1088/1742-6596/864/1/012028

Longitudinal magnetoconductivity and magnetodielectric effect in bilayer graphene

U Zülicke[1,2] and R Winkler[3,4]

[1] School of Chemical and Physical Sciences and MacDiarmid Institute for Advanced Materials and Nanotechnology, Victoria University of Wellington, PO Box 600, Wellington 6140, New Zealand
[2] Kavli Institute for Theoretical Physics, University of California, Santa Barbara, CA 93106, USA
[3] Department of Physics, Northern Illinois University, DeKalb, Illinois 60115, USA
[4] Materials Science Division, Argonne National Laboratory, Argonne, Illinois 60439, USA

E-mail: `uli.zuelicke@vuw.ac.nz`

Abstract. It was recently shown that a finite imbalance between electron densities in the $\mathbf{K}$ and $\mathbf{K}'$ valleys of bilayer graphene induces a magnetoelectric coupling. Here we explore ramifications of this electronically tunable magnetoelectric effect for the optical conductivity and dielectric permittivity of this material. Our results augment current understanding of longitudinal magnetoresistance and magnetocapacitance in unconventional materials.

1. Introduction

The coupling of electric and magnetic degrees of freedom in materials continues to be studied intensely, because of both its interesting physical origin and its potential for useful applications [1–5]. The recent discovery [6, 7] of magnetoelectric couplings in bilayer graphene (BLG) has established an intriguing link between magnetoelectricity and atomically thin materials [8,9]. Here we investigate ramifications of this effect for electric transport, pointing out intriguing similarities, but also crucial differences, with transport characteristics [10–15] arising from the chiral anomaly [16] in Dirac [17] and Weyl [18, 19] semimetals.

As a relevant context, we summarize the basic constitutive relations that represent the chiral magnetic effect [10–16] in Dirac and Weyl semimetals with two valleys characterized by opposite chirality. The most important feature is the generation of a finite imbalance ϱ_v of electron densities between the valleys when both an electric field $\boldsymbol{\mathcal{E}}$ and a magnetic field $\boldsymbol{\mathcal{B}}$ are applied, which also depends on the relaxation time τ_v for inter-valley scattering of charge carriers:

$$\varrho_\mathrm{v} = -\frac{e^3}{2\pi^2\hbar^2}\,\tau_\mathrm{v}\,\boldsymbol{\mathcal{B}}\cdot\boldsymbol{\mathcal{E}} \quad . \tag{1}$$

Combined with the fact that ϱ_v in the presence of a magnetic field causes an electric current $\delta\mathbf{j}$ to flow,

$$\delta\mathbf{j} = -\frac{e}{2\pi^2\hbar^2\,D(E_\mathrm{F})}\,\boldsymbol{\mathcal{B}}\,\varrho_\mathrm{v} \quad , \tag{2}$$

a correction to the magnetoconductivity tensor emerges that is of the form $\delta\underline{\sigma}(\boldsymbol{\mathcal{B}}) = \delta\sigma(\mathcal{B})\,\hat{\boldsymbol{\mathcal{B}}}\hat{\boldsymbol{\mathcal{B}}}$, with

$$\delta\sigma(\mathcal{B}) = \frac{e^4\,\tau_\mathrm{v}}{4\pi^4\hbar^4\,D(E_\mathrm{F})}\,\mathcal{B}^2 \quad . \tag{3}$$

Here $D(E_\mathrm{F})$ denotes the density of states at the Fermi energy E_F. See, e.g., Refs. [10, 12, 14] for relevant derivations and Ref. [20] for a recent experimental observation.

As discussed in greater detail further below, the existence of a magnetoelectric coupling in BLG whose magnitude depends on ϱ_v [6] gives rise to a set of constitutive relations that are similar to those given above for Dirac and Weyl semimetals.

2. Magnetoelectric coupling in BLG for in-plane electric & magnetic fields

For the purpose of the present discussion, we only consider electric fields $\boldsymbol{\mathcal{E}}_\parallel$ and magnetic fields $\boldsymbol{\mathcal{B}}_\parallel$ *parallel to the plane* of the BLG sheet. (Effects of field couplings in the general case are presented in Refs. [6, 7].) The single-particle Hamiltonian describing the charge-carrier dynamics is given by

$$H = H_0(\mathbf{k} + e\boldsymbol{\mathcal{A}}) + e\,\xi_\parallel\,\boldsymbol{\mathcal{E}}_\parallel \cdot \boldsymbol{\mathcal{B}}_\parallel\,\tau_z \quad , \tag{4}$$

where $H_0(\mathbf{k})$ describes the low-energy band structure for the field-free situation in the two valleys associated with the high-symmetry $\mathbf{K}$ and $\mathbf{K}'$ points in the BLG Brillouin zone, and $\boldsymbol{\mathcal{A}}$ is the electromagnetic vector potential. The diagonal Pauli matrix τ_z operates in valley (isospin) space, and $\xi_\parallel$ is a material-dependent parameter quantifying the strength of magnetoelectric coupling.

Several unusual physical effects arise from the presence of the term proportional to $\boldsymbol{\mathcal{E}}_\parallel \cdot \boldsymbol{\mathcal{B}}_\parallel\,\tau_z$. Due to its asymmetric coupling to the $\mathbf{K}$ and $\mathbf{K}'$ valleys, simultaneous application of electric and magnetic fields gives rise to a valley-charge imbalance

$$\varrho_\mathrm{v} \equiv \varrho^{\mathbf{K}} - \varrho^{\mathbf{K}'} = 2e^2\,\xi_\parallel\,D(E_\mathrm{F})\,\boldsymbol{\mathcal{B}}_\parallel \cdot \boldsymbol{\mathcal{E}}_\parallel \quad . \tag{5}$$

This represents an intriguing analogy with the situation in the Dirac or Weyl semimetals, see Eq. (1) above. Furthermore, mirroring phenomena associated with axion electrodynamics [21, 22] or, more generally, with the magnetoelectric effect [23–25], the in-plane magnetic field in conjunction with a finite ϱ_v induces an electric current [6]

$$\delta\mathbf{j} \equiv \mathbf{j}^{\mathbf{K}} + \mathbf{j}^{\mathbf{K}'} = \xi_\parallel\,\boldsymbol{\mathcal{B}}_\parallel\,\partial_t\varrho_\mathrm{v} \quad . \tag{6}$$

While there is some similarity between (6) and the constitutive relation (2) for the Weyl semimetals, there is the crucial difference that the current arising from magnetoelectric coupling in BLG is not proportional to ϱ_v itself but to its time derivative.

3. Magnetotransport from magnetoelectric coupling in BLG

The main focus of the present work is to elucidate how electric-transport characteristics of BLG are modified by the magnetoelectric coupling. Hence, we assume $\boldsymbol{\mathcal{B}}_\parallel$ to be static, but $\boldsymbol{\mathcal{E}}_\parallel$ to be time dependent, $\boldsymbol{\mathcal{E}}_\parallel(t)$. Assuming furthermore spatial uniformity, the continuity equation for ϱ_v becomes

$$\partial_t\varrho_\mathrm{v} + \frac{\varrho_\mathrm{v}}{\tau_\mathrm{v}} = 2e^2\,\xi_\parallel\,D(E_\mathrm{F})\,\boldsymbol{\mathcal{B}}_\parallel \cdot \partial_t\boldsymbol{\mathcal{E}}_\parallel \quad . \tag{7}$$

Straightforward solution using Fourier transformation yields

$$\varrho_\mathrm{v}(\omega) = 2e^2\,\xi_\parallel\,D(E_\mathrm{F})\,\boldsymbol{\mathcal{B}}_\parallel \cdot \boldsymbol{\mathcal{E}}_\parallel(\omega)\;\frac{1}{1 - i/(\omega\tau_\mathrm{v})} \quad . \tag{8}$$

Inserting (8) into the Fourier-transformed Eq. (6), we obtain a contribution to the BLG-sheet conductivity tensor that is due to the magnetoelectric coupling, $\delta\underline{\sigma}(\omega, \boldsymbol{\mathcal{B}}_\parallel) = \delta\sigma(\omega, \mathcal{B}_\parallel)\, \hat{\boldsymbol{\mathcal{B}}}_\parallel \hat{\boldsymbol{\mathcal{B}}}_\parallel$, with

$$\delta\sigma(\omega, \mathcal{B}_\parallel) = -2e^2\, \frac{D(E_\mathrm{F})\, \xi_\parallel^2}{\tau_\mathrm{v}}\, \mathcal{B}_\parallel^2\, \frac{(\omega\tau_\mathrm{v})^2}{\sqrt{1+(\omega\tau_\mathrm{v})^2}}\, \mathrm{e}^{-i\arctan(\omega\tau_\mathrm{v})} \quad . \tag{9}$$

Thus the valley-density-dependent magnetoelectric coupling causes a reduced conductivity in the direction parallel to an applied in-plane magnetic field. The magnitude of the associated response is set by the scale

$$\sigma_\mathrm{ME}(\mathcal{B}_\parallel) = 2e^2\, \frac{D(E_\mathrm{F})\, \xi_\parallel^2}{\tau_\mathrm{v}}\, \mathcal{B}_\parallel^2 \quad , \tag{10}$$

which depends quadratically on $\mathcal{B}_\parallel$ but inversely on τ_v. In the static limit $\omega\tau_\mathrm{v} \ll 1$, the dissipative part of the conductivity dominates but is also suppressed by a small factor $(\omega\tau_\mathrm{v})^2$. The opposite (high-frequency) limit $\omega\tau_\mathrm{v} \gg 1$ is characterized by the conductivity correction being dominantly capacitive with magnitude proportional to the large factor $\omega\tau_\mathrm{v}$, with the dissipative part saturating at $\sigma_\mathrm{ME}(\mathcal{B}_\parallel)$.

4. Magnetodielectric effect in BLG

Using the familiar identity relating the 3D-bulk conductivity and the dielectric permittivity [26], we find a magnetoelectric-coupling-induced change to the dielectric tensor,

$$\frac{\delta\underline{\varepsilon}(\omega, \boldsymbol{\mathcal{B}}_\parallel)}{\varepsilon_0} \equiv i\frac{\delta\underline{\sigma}(\omega, \boldsymbol{\mathcal{B}}_\parallel)}{\varepsilon_0\, \omega\, d} = \frac{\delta\varepsilon(\omega, \mathcal{B}_\parallel)}{\varepsilon_0}\, \hat{\boldsymbol{\mathcal{B}}}_\parallel \hat{\boldsymbol{\mathcal{B}}}_\parallel \quad , \tag{11}$$

$$\frac{\delta\varepsilon(\omega, \mathcal{B}_\parallel)}{\varepsilon_0} = -\frac{2e^2}{\varepsilon_0}\, \frac{D(E_\mathrm{F})\, \xi_\parallel^2}{d}\, \mathcal{B}_\parallel^2\, \frac{\omega\tau_\mathrm{v}}{\sqrt{1+(\omega\tau_\mathrm{v})^2}}\, \mathrm{e}^{i\,\mathrm{arccot}(\omega\tau_\mathrm{v})} \quad . \tag{12}$$

Here d is the electronic width of BLG. Thus this material exhibits a negative in-plane magnetodielectric effect [27, 28] with a magnitude that saturates at the susceptibility scale

$$\chi_\mathrm{ME}(\mathcal{B}_\parallel) = \frac{2e^2}{\varepsilon_0}\, \frac{D(E_\mathrm{F})\, \xi_\parallel^2}{d}\, \mathcal{B}_\parallel^2 \tag{13}$$

in the high-frequency limit $\omega\tau_\mathrm{v} \gg 1$ but which acquires a prefactor $\omega\tau_\mathrm{v}$, and therefore vanishes, in the static limit $\omega\tau_\mathrm{v} \ll 1$. The imaginary part of the dielectric function exhibits the lineshape of the derivative of a Lorentzian, thus its measurement would allow convenient extraction of the inter-valley relaxation time τ_v. See Fig. 1 for an illustration of the frequency dependencies exhibited by the real and imaginary parts of the contributions to the conductivity and the dielectric constant due to the magnetoelectric effect.

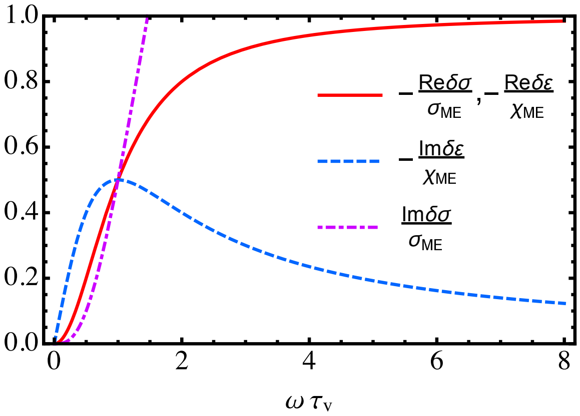

Figure 1. Frequency dependence of the real and imaginary parts of the contribution $\delta\sigma$ to the longitudinal sheet conductivity in BLG and the contribution $\delta\varepsilon$ to the dielectric constant arising due to the valley-density-dependent magnetoelectric effect. τ_v is the inter-valley relaxation time.

5. Discussion and conclusions

Our study has revealed the existence of a longitudinal magnetoconductivity and an associated magnetocapacitance in BLG arising from its valley-density-dependent magnetoelectric effect. More broadly, this behavior will be exhibited also by other materials whose symmetries are similar to BLG. The ability to generate a valley-density imbalance ϱ_{v} by simultaneously applied non-orthogonal electric and magnetic fields constitutes an intriguing analogy between BLG and the Dirac and Weyl semimetals. Furthermore, in both material classes, a magnetic field causes electric current to flow when the valley densities are unequal, but this imbalance must also be time-varying in BLG whereas a current is generated already by a static ϱ_{v} in Dirac and Weyl semimetals. Thus, while the unusual magnetotransport properties emerging in BLG and those associated with the chiral anomaly in Dirac and Weyl semimetals turn out to share certain features, they have a fundamentally different origin and also exhibit different dependencies on physical parameters such as the inter-valley relaxation time.

Acknowledgments

UZ thanks M. S. Fuhrer, I. Martin, and J. E. Moore for useful discussions and acknowledges support from NSF Grant No. PHY11-25915 while at the Kavli Institute for Theoretical Physics. RW was supported by the NSF under grant No. DMR-1310199. Work at Argonne was supported by DOE BES under Contract No. DE-AC02-06CH11357.

References

[1] Fiebig M 2005 *J. Phys. D* **38** R123–52
[2] Ramesh R and Spaldin N A 2007 *Nat. Mater.* **6** 21–9
[3] Khomskii D 2009 *Physics* **2** 20
[4] Kimura T 2012 *Annu. Rev. Condens. Matter Phys.* **3** 93–110
[5] Dong S, Liu J, Cheong S and Ren Z 2015 *Adv. Phys.* **64** 519–626
[6] Zülicke U and Winkler R 2014 *Phys. Rev. B* **90** 125412
[7] Winkler R and Zülicke U 2015 *Phys. Rev. B* **91** 205312
[8] Novoselov K S, Jiang D, Schedin F, Booth T J, Khotkevich V V, Morozov S V and Geim A K 2005 *Proc. Natl. Acad. Sci. USA* **102** 10451–53
[9] Xu M, Liang T, Shi M and Chen H 2013 *Chem. Rev.* **113** 3766–98
[10] Zyuzin A A and Burkov A A 2012 *Phys. Rev. B* **86** 115133
[11] Grushin A G 2012 *Phys. Rev. D* **86** 045001
[12] Son D T and Spivak B Z 2013 *Phys. Rev. B* **88** 104412
[13] Vazifeh M M and Franz M 2013 *Phys. Rev. Lett.* **111** 027201
[14] Burkov A A 2015 *Phys. Rev. B* **91** 245157
[15] Goswami P, Pixley J H and Das Sarma S 2015 *Phys. Rev. B* **92** 075205
[16] Nielsen H and Ninomiya M 1983 *Phys. Lett. B* **130** 389–96
[17] Yang B J and Nagaosa N 2014 *Nat. Commun.* **5** 4898
[18] Vafek O and Vishwanath A 2014 *Annu. Rev. Condens. Matter Phys.* **5** 83–112
[19] Hasan M Z, Xu S Y and Bian G 2015 *Phys. Scr.* **T164** 014001
[20] Xiong J, Kushwaha S K, Liang T, Krizan J W, Hirschberger M, Wang W, Cava R J and Ong N P 2015 *Science* **350** 413–16
[21] Wilczek F 1987 *Phys. Rev. Lett.* **58** 1799–802
[22] Franz M 2008 *Physics* **1** 36
[23] Hehl F W, Obukhov Y N, Rivera J P and Schmid H 2008 *Phys. Lett. A* **372** 1141–46
[24] Qi X L, Hughes T L and Zhang S C 2008 *Phys. Rev. B* **78** 195424
[25] Essin A M, Turner A M, Moore J E and Vanderbilt D 2010 *Phys. Rev. B* **81** 205104
[26] Jackson J D 1999 *Classical Electrodynamics* 3rd ed (Hoboken, NJ: Wiley) Section 7.5 C
[27] Kimura T, Kawamoto S, Yamada I, Azuma M, Takano M and Tokura Y 2003 *Phys. Rev. B* **67** 180401
[28] Singh M P, Prellier W, Simon C and Raveau B 2005 *Appl. Phys. Lett.* **87** 022505